RESPONSES OF STRUCTURE CLUSTERS TO A NEAR-FAULT EARTHQUAKE

Tielin Liu
School of Civil Engineering, Shenyang Jianzhu University, Shenyang, 110168, China

Yu Luan & Wei Zhong
School of Civil Engineering, Dalian University of Technology, Dalian, 116024, China

SUMMARY:
An integrated method, in which the structures, earth media, and causative fault are considered together in the practical calculation, is presented for simulating the responses of structure clusters to a near-fault earthquake. The multi-degree-of-freedom model is adopted for the multi-story structure and the source model of finite fault is applied for the causative fault. Three types of investigated lumps are respectively used for the structures, the earth medium, and the connections between them to simulate wave propagation in the structures and in the earth medium simultaneously. The earthquake responses are studied for three clusters of 6-story plane frame structures, which respectively located on the hanging wall, rupture forward, and footwall of the fault. The inter-story drifts and the dynamic deformations of the frame structures are provided. The results show the earthquake-response characteristics of structures near the causative fault.

Keywords: Earthquake response; structure cluster; Near-fault earthquake; Investigated lump

1. INTRODUCTION

After the 1985 Mexico earthquake, researchers began to study the problems of site-city interaction (SCI) (Wirgin and Bard, 1996; Semblat et al, 2008; Boutin and Roussillon, 2004; Tsogka and Wirgin, 2003). In these investigations about SCI, the city was usually modeled as an assembly of homogeneous blocks or a group of equivalent single-degree-of-freedom oscillators resting on inhomogeneous half-space excited by incident plane wave.

For a city area subjected to a near-fault earthquake, the influences of fault-rupture process on the earthquake responses of structures should be considered. It is known that the finite-fault source is an appropriate mechanism of seismic source for the near-fault earthquake (Hartzell, 1978; Heaton and Hartzell, 1989; Somerville et al, 1991; Liu et al, 2012). Therefore, it is better to introduce finite-fault model for simulating the responses of structures in the city during a near-fault earthquake.

In this paper, an integrated method is presented for studying the responses of structure clusters during a hypothetical near-fault earthquake. We study in detail a numerical example, which integrate the causative fault, the earth medium and the structure clusters located respectively at the epicenter

(hanging wall), rupture forward, and footwall of the earthquake fault.

2. MODEL OF STRUCTURES, EARTH MEDIUM AND A NEAR-FAULT THRUST FAULT

Fig. 1 is the sketch of the model of planar RC frame structures, earth medium and finite fault for two-dimensional problem. In Fig. 1 (c), the inclined dark line shows the causative fault with a dip angle of 40° and its top being 2km beneath the ground surface. Three structure clusters on the ground surface are respectively located at the epicenter (hanging wall), rupture forward, and footwall of the earthquake fault. Three stars denote the locations of subsources. The structures are shown by using the small grey rectangles connecting to the horizontal solid line. Each cluster consists of thirty 6-story 3-span RC plane frame structures with equal interval of 22m. The distance between the centers of adjacent clusters is 6.9km. Fig. 1 (a) shows the computational model of a RC frame structure and Fig. 1 (b) shows one plane frame structure. The height of every story is 3m, the mass of the roof is 3.21×10^4 Kg, and the mass of every other floor is 3.59×10^4 Kg. The section size of columns is 500mm×500mm. The lateral stiffness and vertical stiffness of every story of the plane frame structure are 2.59×10^5KN/m and 2.8×10^7KN/m, respectively.

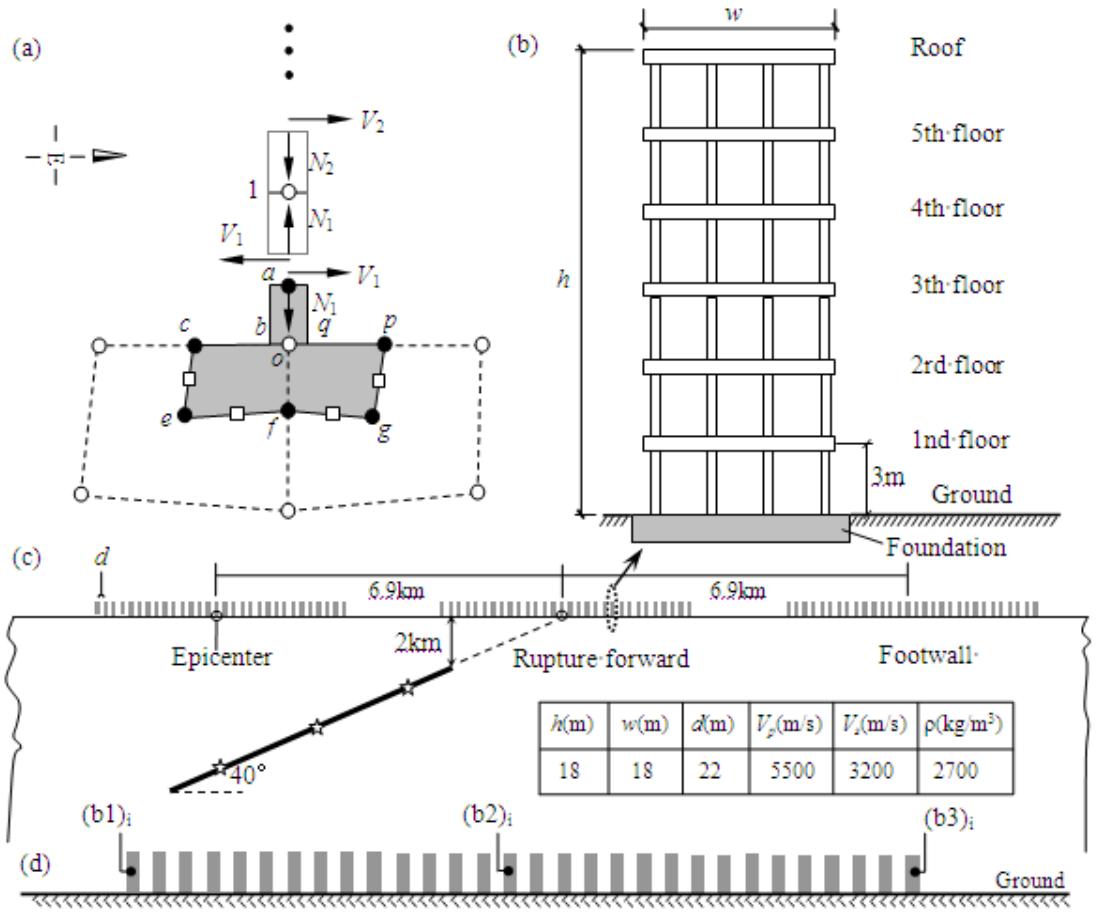

Figure 1. The calculation model integrated 6-storey RC frame structures, earth medium and the causative fault. $(b1)_i$, $(b2)_i$ and $(b3)_i$ are used for outputting the inter-story drifts between the second floor and third floor; Subscript i=1 denotes structures at the epicenter, i=2 for the rupture forward and i=3 for the footwall.

3. SIMULATION ALGORITHM

Three types of investigated lumps are considered for the structures, the earth medium, and the connections between them. The first type of investigated lump is in the RC plane frame structures, the second type in the half-space and the third type for connecting the structure to the earth medium.

3.1 Algorithm for Simulating Wave Propagation in Structures

3.1.1 Governing equations

One of the first type investigated lumps is composed of the rigid slab of i th floor and all of the half columns connected to the rigid slab, for example, the investigated lump 1 in Fig. 1(a). Assuming the accelerations being equal within the investigated lump, then the acceleration of i th slab can be used to characterize the acceleration of investigated lump i .

The dynamic equilibrium equations of the i th investigated lump are as follows (see Fig. 1(a)):

$$m_i \ddot{u}_{xi} = V_i - V_{i-1} \tag{1}$$

$$m_i \ddot{u}_{zi} = N_{i-1} - N_i \tag{2}$$

where $\ddot{u}_{xi}$ and $\ddot{u}_{zi}$ are respectively the horizontal and vertical accelerations of investigated lump i . m_i is the mass. V_i and V_{i-1} are respectively the inter-story shear forces, and N_i and N_{i-1} are respectively the inter-story axial forces.

The shear force (Clough and Penzien, 1975) and axial force can be calculated as follows:

$$V_i = k_{li}[u_{xi+1} - u_{xi}] \tag{3}$$

$$N_i = k_{ci}[u_{zi} - u_{zi+1}] \tag{4}$$

where $k_{li} = \sum_{j=1}^{n_c} 12(EI)_j / h_i^3$ and $k_{ci} = \sum_{j=1}^{n_c} (EA)_j / h_i$ is respectively the lateral and vertical stiffness of the total columns of i th story. $(EI)_j$ and $(EA)_j$ is the bending and compressive stiffness of j th column belong to the i th story. n_c is the total number of the columns of the i th story, and h_i is storey height. u_{xi} and u_{xi+1} are respectively the displacement of i th and $(i+1)$ th investigated

lumps in horizontal direction, and u_{zi} and u_{zi+1} are the ones in vertical direction.

3.1.2 Implementation

When the displacement components u_{xi}^t and u_{zi}^t at time t have been calculated, then shear forces V_i^t, V_{i-1}^t and axial forces N_i^t, N_{i-1}^t acting on the investigated lump can be obtained by Eqns. (3) and (4) at time t. Substituting the shear forces and the axial forces into Eqns. (1) and (2), the acceleration components $\ddot{u}_{xi}^t$ and $\ddot{u}_{zi}^t$ at time t can be obtained. The displacement components $u_{xi}^{t+\Delta t}$ and $u_{zi}^{t+\Delta t}$ of the ith investigated lump at the time $t+\Delta t$ can be obtained by using time integration. Implementing the above circulating procedure in recursive manner, the displacements, accelerations, shear forces, and axial forces of the structures can be updated from time t to time $t+\Delta t$ by the computer program. Thus the wave propagations can be implemented within the structures in order to provide the seismic responses of structures.

3.2 Algorithm for Complementing Wave Propagation Between Structure and Earth Medium

3.2.1 Governing equations

In order to simulate the two-way wave propagation between the earth medium and the structures, the connecting investigated lump is constructed for linking the columns of frame structures to the earth medium. The foundations of structures and the earth medium are assumed to be joined together rigidly in this paper.

Fig. 1(a) shows the connecting investigated lump o that is made up of half columns of the 1st story of the frame structure and the earth medium (see the enclosed segments *a-b-c-e-f-g-p-q-a*). This investigated lump is subjected to shear and axial forces from its above investigated lump and the distributed forces on segments of line *c-e-f-g-p* from the surrounding investigated lumps in earth medium. The acceleration of node o is used to characterize the acceleration of the investigated lump.

The dynamic equilibrium equations of investigated lump o are as follows:

$$M_o\ddot{u}_{xo} = f_x + V_1 \tag{5}$$

$$M_o\ddot{u}_{zo} = f_z - N_1 \tag{6}$$

where M_o is the mass of investigated lump o. $\ddot{u}_{xo}$ and $\ddot{u}_{zo}$ are the accelerations of investigated lump o in x and z directions respectively. f_x and f_z are the forces from the surrounding investigated lumps in earth medium. V_1 and N_1 are the shear force and axial force exerted on

investigated lump o. We have

$$V_1 = k_{l1}(u_1 - u_o) \tag{7}$$

$$N_1 = k_{c1}(w_o - w_1) \tag{8}$$

where k_{l1} and k_{c1} are the lateral stiffness and vertical stiffness of the total columns of the first story. u_o and w_o are , respectively, the horizontal and the vertical displacements of investigated lump o.

3.2.2 implementation

When the displacement components u_{xo}^t and u_{zo}^t at time t have be calculated, then shear force V_1^t and axial force N_1^t can be obtained by Eqns. (3) and (4), and f_x^t and f_z^t around node o at time t can be given by using the same algorithm as in the authors' former published paper (Liu et al, 2012). Using Eqns. (5) and (6), acceleration components $\ddot{u}_{xo}^t$ and $\ddot{u}_{zo}^t$ of investigated lump o can be calculated. Thus the displacement components $u_{xo}^{t+\Delta t}$ and $u_{zo}^{t+\Delta t}$ at time $t+\Delta t$ can be obtained by using time integration.

It should be pointed that because of the limit of paper length, the calculating algorithm for simulating wave propagation in earth medium (Liu et al, 2012) has not been introduced herein.

Combining Sections 3.1 and 3.2 with the authors' algorithm for wave propagation in earth medium (Liu et al, 2012), the displacements, accelerations, stress components in earth medium, shear forces and axial forces in structures can be updated from time t to time $t+\Delta t$.

Circulating the procedure mentioned above in recursive manner in time domain, the algorithm is presented for simulating the wave propagation in structures and earth medium simultaneously.

3.3 Implementation of Sources of Causative fault

The width of causative fault can be calculated by using the empirical relationships given by Wells and Coppersmith (1994). That is, the rupture area A and rupture length L can be respectively calculated by

$$\log A = -3.49 + 0.91M_w \tag{9}$$

$$\log L = -1.88 + 0.5M_w . \tag{10}$$

Then the rupture width of the causative fault can be obtained by using the rupture area A divided by the rupture length L.

Using the empirical relationship (Beresnev and Atkinson, 2002) between the subfault size and moment magnitude

$$\log \Delta l = -2.0 + 0.4M_w \quad (\text{for } 4 \le M_w \le 8), \tag{11}$$

we can obtain the subfault length Δl (in km) along the dip direction of the fault. Then the scalar seismic moment can be calculated by

$$M_{0i} = \mu_i u_i(t) \Delta l \tag{12}$$

for the plane strain problem (Liu et al, 2012). μ_i is shear modulus and $u_i(t)$ is slip displacement at time t. Here i denotes the i th subfault.

In this study, we adopt the displacement-time function (Beresnev, 2001) as follows:

$$u_i(t) = u_i(\infty)[1 - (1 + t/\tau)e^{-t/\tau}], \tag{13}$$

where τ is the rise time and $u_i(\infty)$ is the final value of slip displacement of subfault i.

When the final slip displacements and rise times are assumed to be equal for all the subfaults, we have (Wells and Coppersmith, 1994; Somerville et al, 1993)

$$\log\ u(\infty) = -0.74 + 0.08M_w \quad (\text{for } 5.8 \le M_w \le 7.4) \tag{14}$$

$$\tau = 1.72 \times 10^{-9} \times (M_0)^{1/3} \tag{15}$$

where seismic moment $M_0 = 10^{1.5(M_w + 10.7)}$ in dyne-cm (Hanks and Kanamori, 1979) and M_w is the moment magnitude.

The fault rupture starts from the hypocenter inside a subfault and propagates outwards. Let the initial rupture starting from the center of subfault i_0, the delay time t_{0i} of the other subfaults can be calculated by

$$t_{0i} = [(i - i_0)\sqrt{dx^2 + dz^2}\,]/V_R \tag{16}$$

where $V_R = 0.8V_s$ is the rupture velocity. V_s is the shear-wave velocity (Beresnev and Atkinson, 2002); $i = 1,...,n_s$ and n_s is the number of subfaults. dx and dz are projections of the interval of adjacent subfaults in x and z directions respectively.

A double-couple source is applied on each subfault in the mechanism of finite-fault source. For the plane strain problem with its calculation plane perpendicular to the strike direction, the force components to describe the double-couple source can be given as follows (Liu et al, 2012):

$$\begin{cases} f_{xxi} = M_{xxi}/6\Delta x \\ f_{zzi} = M_{zzi}/6\Delta z \\ f_{xzi} = M_{xzi}/6\Delta x; \quad f_{zxi} = M_{xz}/6\Delta z \end{cases} \tag{17}$$

where Δx and Δz are the spatial-discrete intervals in x and z directions respectively. $M_{xxi} = -M_{0i}\sin\lambda\sin 2\delta$, $M_{xzi} = M_{zxi} = M_{0i}\sin\lambda\cos 2\delta$ and $M_{zzi} = M_{0i}\sin\lambda\sin 2\delta$ are the components of moment tensor of subfault i where λ is the rake angle and δ the dip angle of the fault (Aki and Richards, 1980).

4. EARTHQUAKE RESPONSES OF STRUCTURE CLUSTERS NEAR FAULT

In this study, a hypothetical earthquake of M_w 6.0 is adopted to study the phenomenon of wave propagation in the structures and the earth medium simultaneously. The subfault length Δl of 2.5km is obtained by using Eqns. (9), (10) and (11). Using Eqns. (14) and (15), the final value of slip displacement and the rise time for every subfault are given to be 0.55m and 0.38s respectively. The parameters of earth medium are shown in Fig. 1 (c). The receivers for one structure cluster are shown in Fig. 1 (d) to measure the inter-story drifts between the second floor and third floor (see $(b1)_i$, $(b2)_i$,$(b3)_i$). In practical calculation, spatial step of 20m is used. Time step is 2ms and the total computational time is 30s.

Fig. 2 shows the time-histories of inter-story drifts between the second floor and third floor of structures located on the hanging wall, rupture forward, and footwall of the causative fault respectively. Obviously, the inter-story drifts located on the hanging wall of the fault are larger than those of structures located on the rupture forward and the footwall of the fault. The maximum inter-story drift on the rupture forward and the footwall are respectively 35.2% and 23.4% of that on hanging wall of the fault. The inter-story drifts also show the “hanging wall effect”.

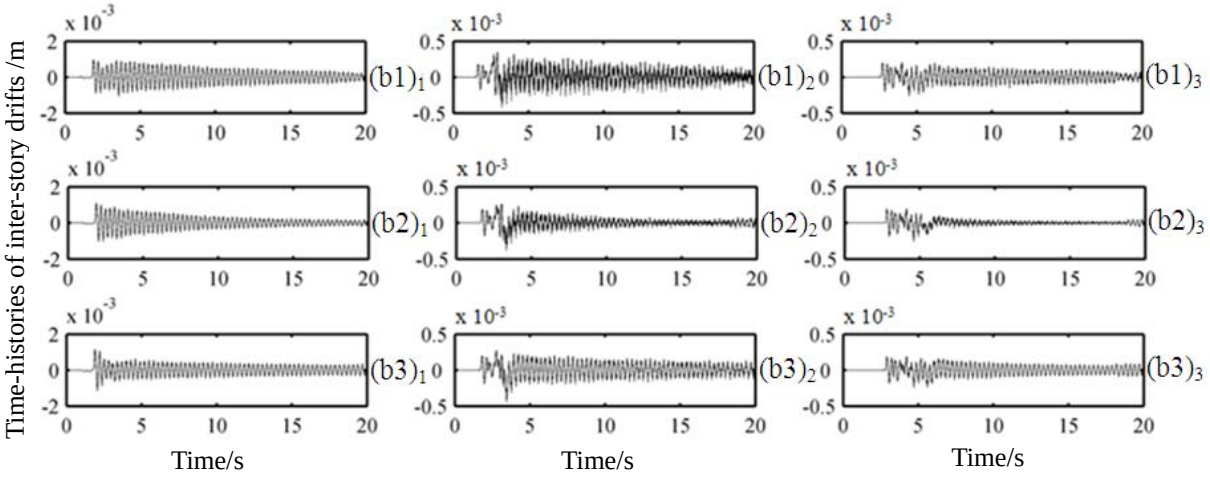

Figure 2. Time-histories of inter-story drifts of structures located on the hanging wall (left), rupture forward (middle), and footwall (right) of the causative fault. Subscript 1 denotes structures being on the hanging wall, and subscripts 2 and 3 are respectively for the rupture forward and the footwall.

Fig. 3 shows the wavefields of horizontal accelerations at 1.6s and 2.8s. The propagating process of fault rupture can be seen clearly in the two figures. Snapshot at 1.6s shows the *P* - and *SV* -wave fields of the initial and second double-couple sources on the fault plane. Snapshot at 2.8s show the whole triggered process of three subfaults and the successive creations of *P* - and *SV* -wave radiated from each subfault. The Doppler effects can be seen clearly from the snapshots because of the movements of subsources.

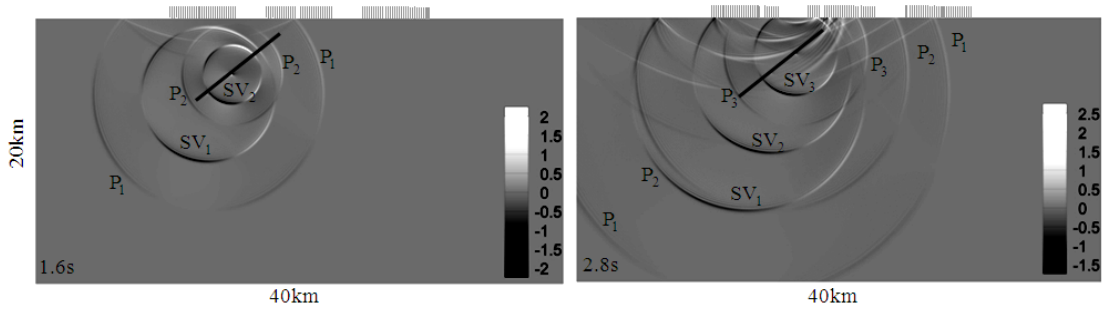

Figure 3. Snapshots of wave-field of horizontal acceleration (unit in m/s^2) at 1.6s and 2.8s respectively. Thick solid lines denote the causative fault buried below the city. The wave-field area is 40km × 20km with three structure clusters on the top of it.

Fig. 4 shows snapshots of the horizontal displacements of structures located on the hanging wall, the rupture forward, and the footwall of the causative fault at different time. Fifteen structures extracted from one cluster of 6-story plane frame structures are used to show the responses of structure clusters. In the figures, “0” denotes the center of the first structure and “1120” the twenty-ninth structure from the left in the original configuration. In order to show the deformations of structure clusters clearly, the absolute values of horizontal displacements of the foundations are amplified 100 times, the relative values of the floors to their own foundations are amplified 500 times for the structures located on the

hanging wall, and 700 times for the structures located on the rupture forward and the footwall.

The structure cluster on the hanging wall moves back and forth as a whole during the hypothetical earthquake. However, the deformations are irregular for the structures on the rupture forward as well as the footwall, especially for the structures on the rupture forward.

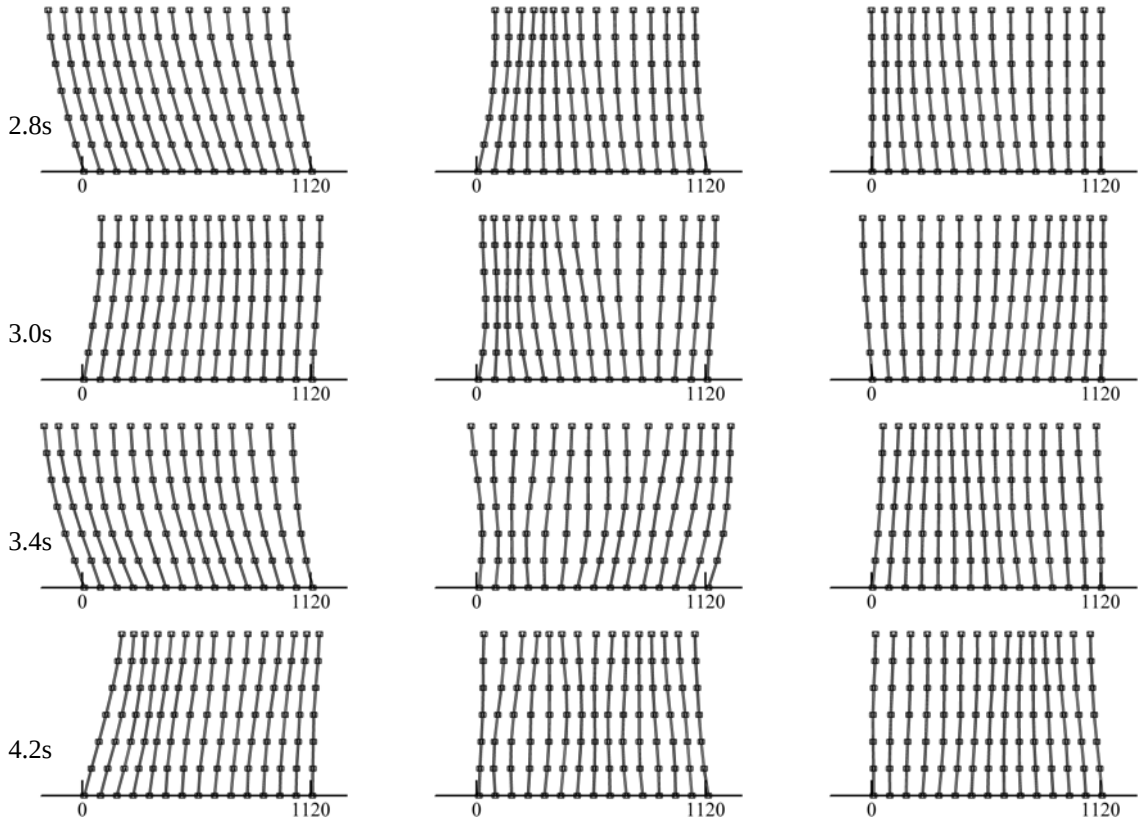

Figure 4. Snapshots of the horizontal deformations of structures located on the hanging wall (left), the rupture forward (middle), and the footwall (right) respectively during the hypothetical earthquake at different times. Small squares denote the floors of structures.

5. CONCLUSIONS

An integrated method based on the concept of investigated lump is presented for simultaneously simulating wave propagation in structures and earth medium during fault rupture. The structures, earth media, and causative fault are considered together to simulate the earthquake process in the practical calculation. The numerical results show that the inter-story drifts of frame structures located on the hanging wall of the fault are much larger than those of the structures located on the rupture forward and footwall. The dynamic deformations of structures on the rupture forward are quite irregular during earthquake. The adjacent structures sometimes approach each other and sometimes separate from one another. It demonstrates that if two buildings on the rupture forward are built close to each other, they might collide during an actual earthquake because of the irregular vibrations of buildings. The proposed method and the cognitions obtained in this paper are expected to be helpful for the mitigation

of earthquake disaster, the land-using plan in the earthquake-prone cities.

ACKNOWLEDGEMENT

Project 10972144 supported by National Natural Science Foundation of China.

REFERENCES

Aki, K. and Richards, P. (1980). Quantitative seismology: theory and methods. San Francisco: W. H. Freeman and Company.

Boutin, C and Roussillon, P. (2004). Assessment of the urbanization effect on seismic response, *Bulletin of Seismological Society of America*. 94: 251-268.

Beresnev, I. A. (2001). What we can and cannot learn about earthquake sources from the spectra of seismic waves. *Bulletin of Seismological Society of America*. 91: 397-400.

Beresnev, I. A. and Atkinson, G. M. (2002). Source parameters of earthquakes in eastern and western North America based on finite-fault modeling. *Bulletin of Seismological Society of America*. 92: 695-710.

Clough, R. W. and Penzien, J. (1975). Dynamics of structures. New York: McGraw-Hill.

Hanks, T. C. and Kanamori, H. (1979). A moment magnitude scale. *Journal of Geophysical Research*. 84: 2348-2350.

Hartzell, S. H.(1978). Earthquake aftershocks as Green's functions. *Geophysical Research Letters*. 5: 1-4.

Heaton, T. H. and Hartzell, S. H. (1989). Estimation of strong ground motions from hypothetical earthquakes on the Cascadia subduction zone, Pacific Northwest. *Pure and Applied Geophysics*. 129: 131-201.

Liu, T., Luan, Y. and Zhong, W. (2012). A numerical approach for modeling near-fault ground motion and its application in the 1994 Northridge earthquake. *Soil Dynamics and Earthquake Engineering*. 34: 52-61.

Semblat, J. F., Kham, M. and Bard, P. Y. (2008). Seismic-wave propagation in Alluvial basins and influence of site-city interaction. *Bulletin of Seismological Society of America*. 98: 2665-2678.

Somerville, P. G., Sen, M. and Cohee, B. (1991). Simulations of strong ground motions recorded during the 1985 Michoacan, Mexico and Valparaiso, Chile, earthquakes, *Bulletin of Seismological Society of America*. 81: 1-27.

Somerville, P. G., Irikura, K., Sawada, S., Iwasaki, Y., Tai, M and Fushimi, M. (1993). Characterizing earthquake slip models for the prediction of strong ground motion. *Proceedings of the 22 JSCE earthquake engineering symposium, Japan Society of Civil Engineering*. 291-294.

Tsogka, C and Wirgin, A. (2003). Simulation of seismic response in an idealized city. *Soil Dynamics and Earthquake Engineering*. 23: 391-402.

Wells, D. L. and Coppersmith, K. J. (1994). New empirical relationships among magnitude, rupture length, rupture width, rupture area, and surface displacement. *Bulletin of Seismological Society of America*. 84: 974-1002.

Wirgin, A. and Bard, P. Y. (1996). Effects of buildings on the duration and amplitude of ground motion in Mexico City. *Bulletin of Seismological Society of America*. 86: 914-920.